

Nonlinear Aerodynamics of Two-Dimensional Airfoils in Severe Maneuver

James E. McCune* and Chun-Ming G. Lam†

Massachusetts Institute of Technology, Cambridge, Massachusetts
and

Matthew T. Scott‡

Bell Helicopter Textron, Fort Worth, Texas

This paper presents a nonlinear theory of the incompressible aerodynamics of two-dimensional airfoils in unsteady potential flow. Results are obtained for cases of both large and small amplitude motion. The analysis, which is based in part on an extension of Wagner's integral equation to the nonlinear regime, allows completely for the trailing wake's tendency to deform under local velocities. Interactive computational results are presented for a variety of imposed airfoil motions. These show examples of wake-induced lift and moment augmentation and/or delay on the order of 20–30 percent of quasistatic values as well as a variety of long-term "history" effects. The expandability and flexibility of the present computational method in the online mode are noted, as well as the relative speed with which solutions are obtained.

Nomenclature

c	= airfoil chord length
$h(t)$	= height of airfoil midchord above reference axis
$L(t), M(t)$	= lift and moment on the airfoil
s	= distance along the wake from the airfoil trailing edge
$s_{\max}(t)$	= distance along the wake up to the end of the wake
t	= time
\bar{U}	= $U_{\infty} + \dot{h} \tan \alpha$
U_{∞}	= freestream speed
$\hat{u}(\beta)$	= total tangential velocity component on the airfoil
$\hat{u}_w(\beta)$	= wake-induced tangential velocity on the airfoil
u, v	= Cartesian velocity in inertial airfoil frame components
$\hat{v}(\beta)$	= total normal velocity component on the airfoil
$\hat{v}_w(\beta)$	= wake-induced normal velocity on the airfoil
x, y	= Cartesian coordinates fixed on global reference axes in the physical (airfoil) plane
\hat{x}, \hat{y}	= Cartesian coordinates parallel and normal to the airfoil
z, \hat{z}	= complex equivalents $x + iy, \hat{x} + i\hat{y}$
$z_v(s, t)$	= vortex location in the wake, $x_v + iy_v$
$\alpha(t)$	= angle of attack
$\gamma(\beta)$	= total strength of bound vorticity on the airfoil
$\gamma_0(\beta)$	= strength of bound vorticity if wake absent
$\gamma_1(\beta)$	= strength of additional bound vorticity needed because of wake
$\gamma_w(s, t)$	= strength of free vorticity in the wake
$\Gamma_0(t)$	= bound circulation, if wake absent. $\Gamma_0 = \int_{-c/2}^{c/2} d\hat{x} \gamma_0$
$\Gamma_1(t)$	= additional bound circulation needed because of wake. $\Gamma_1 = \int_{-c/2}^{c/2} d\hat{x} \gamma_1$
$\Gamma_{\text{airfoil}}(t)$	= total bound circulation, $\Gamma_0 + \Gamma_1$

$\Gamma_{\text{wake}}(t)$	= total circulation of the free wake
$\lambda, \bar{\lambda}$	= nonlinear shifted times, $t - \tau, t - \bar{\tau}$
ρ_{∞}	= density
$\tau, \bar{\tau}$	= drift times
φ	= velocity potential

Introduction

THE early, classical studies of the aerodynamic response of an airfoil to unsteady motion, including the effects of the airfoil's unsteady wake, were carried out in such pioneering works as those of Theodorsen,¹ von Kármán,² Küssner,³ Sears,⁴ and Wagner.⁵ These original contributions were based on potential flow principles and in part on a set of linearizing assumptions that restricted their applicability to low-amplitude airfoil motions and small angles of attack. Among the corresponding limitations in these classical studies are the approximations that the wake be laid out flat behind the airfoil and that the vorticity within it be convected as if by the freestream.

In this paper, with help from the computer and computer graphics, we address the nonlinear case of large-amplitude airfoil motion and attempt to show that this can be done essentially as an extension of classical analytical techniques despite the occurrence of severe wake deformation and roll-up. The overall results obtained are similar in form and spirit to those of other modern studies, cited below, which also include the effects on nonlinear wake deformation. But an attempt is made in this work to reduce computational effort to a minimum by extending the classical theory's analytical methods as far as possible.

In the present treatment, for example, an extension of Wagner's integral equation^{2,5} to the nonlinear case is obtained, enabling us to relate the exact circulation strength of each wake element as it enters the wake to the sequential development of the airfoil circulation. That element's circulation is then fixed for all time as it convects with the distorted wake. In addition, the location of each such wake element is described conveniently in terms of characteristic coordinates, including the "shifted time" discussed below. The resulting procedure provides an analytic framework within which a relatively simple and rapid computer code can be developed, depicting airfoil response to a given maneuver.

Using this code with computer graphics, one can determine the wake convection quite quickly, enabling one to see the wake unfold as the program runs. Output of loading, force, and moment histories is also generated and can be displayed

Presented as Paper 88-0129 at the 26th AIAA Aerospace Sciences Meeting, Reno, NV, Jan 11–14, 1988; received May 20, 1988; revision received Oct. 14, 1988. Copyright © 1988 American Institute of Aeronautics and Astronautics, Inc. All rights reserved.

*Professor, Department of Aeronautics and Astronautics. Associate Fellow AIAA.

†Research Assistant, Department of Aeronautics and Astronautics.

‡Engineer, Aerodynamic Technology.

online. A typical run for a given maneuver occupies times from only a few minutes to half an hour per case on a VAX 11-750, depending on the time step and/or wake resolution required.

Kinematics of Nonlinear Wake Convection

One of the keys to our procedure is the effective nonlinear description of vortex convection within the wake. For this purpose a method based on characteristic variables is introduced.

Any free vorticity associated with unsteady plane two-dimensional fluid motion in the incompressible limit obeys the Helmholtz Law in the form $d\Omega_z/dt = 0$. Formally, therefore, if $A^{(1)} = \lambda(x, y, t)$ and $A^{(2)} = \eta(x, y, t)$ are two independent characteristic solutions of $dA^{(n)}/dt = 0$, with appropriate boundary and initial conditions, then $\Omega_z(x, y, t) = \Omega_z(\eta, \lambda)$.

Boundary conditions can be specified such that one of these characteristic variables, η say, is constant on streaklines (and thus on the airfoil "wake") drawn at fixed t . The remaining variable, λ , can then be chosen to be the shifted time

$$\lambda \equiv t - \tau \quad (1)$$

where

$$\frac{d\tau}{dt} = 1 \quad (2)$$

and τ is the Eulerian "drift time" with the usual simple physical interpretation.⁶ Extension of this classical procedure to three-dimensional convection is straightforward.

When a concentrated vortex sheet is embedded in otherwise potential flow the variables η and λ defined above will generally be discontinuous at the sheet. In that case it is useful to replace η by a continuous function, η_c , say, which instead of $d\eta/dt = 0$ satisfies

$$\left. \begin{aligned} \frac{d\eta_c}{dt} &\equiv \frac{\partial \eta_c}{\partial t} + \langle v \rangle \cdot \nabla \eta_c = 0 \\ \Delta v \cdot \nabla \eta_c &= 0 \end{aligned} \right\} \quad (3)$$

and

The statement $\eta_c(x, y, t) = \text{constant}$ then describes a sheet (or streakline) whose deformation is controlled by convection at the mean velocity at the sheet:

$$\langle v \rangle \equiv \frac{1}{2} (v^+ + v^-) \quad (4)$$

Also, Eq. (3b) states that the velocity jump

$$\Delta v \equiv v^+ - v^- \quad (5)$$

has no component perpendicular to the sheet at any time, which is one of the boundary conditions appropriate to evolution of a free vortex sheet.

In the same framework the second characteristic variable needed at and along the sheet can be chosen to be the "mean shifted time"

$$\bar{\lambda} \equiv t - \bar{\tau} \quad (6)$$

in analogy with Eq. (1). In this case, however,

$$\frac{d\bar{\tau}}{dt} = \frac{\partial \bar{\tau}}{\partial t} + \langle v \rangle \cdot \nabla \bar{\tau} = 1 \quad (7)$$

where $\bar{\tau}$ represents the mean drift time of fluid elements within the vortex sheet.

The variable $\bar{\lambda}$ provides the coordinate along the wake; in fact, it identifies each fluid element in the wake according to when it left a specified upstream location such as the airfoil trailing edge. For the classical theory with *linearized* wake convection at freestream speed U_∞ , for example, this shifted time is simply

$$\bar{\lambda} = t - \frac{x - c}{U_\infty} \quad (\text{linear limit})$$

In the classical theory, as described in Ref. 2, for example, major advantage is taken of the fact that the wake vorticity is a pure function of $\bar{\lambda}$ (linear). In the present nonlinear treatment the same idea is exploited using the nonlinear variable in Eqs. (6) and (7).

Dynamics of Free Wake Convection

If the flow is potential on either side of the vortex sheet, then the potential jump $\Delta\varphi$ occurring at the sheet is a function of both x and t , which must be determined or specified. In the present case application of the Bernoulli equation on either side of the sheet, together with the boundary condition that there be no jump in static pressure across the sheet, yields the restriction $d\Delta\varphi/dt \equiv \partial\Delta\varphi/\partial t + \langle v \rangle \cdot \nabla \Delta\varphi = 0$. [The relation determining " $\Delta\varphi$ " emphasizes the fact that in the presence of a deforming unsteady wake, the boundary-value problem we must solve for φ is inherently nonlinear even for the irrotational, solenoidal case. In effect, unlike the classical treatment, we must satisfy the condition $\Delta p = 0$ on a surface (the wake) whose shape and location is to be determined as part of the solution. Nevertheless, in our present numerical time-stepping procedure we are able to retain a certain "linear" feature to our approach. At each time step, namely, we are able to regard the wake surface as "known" at that instant, just after its relocation during the previous time step.] As a result, we can write, all along the wake in the two-dimensional case,

$$\Delta\varphi = \Delta\varphi(\bar{\lambda}) \quad (8)$$

Thus, the $\Delta\varphi(x, t)$ at the wake is a function of the single characteristic variable, $t - \bar{\tau}(x, t)$, and the statement $\Delta\varphi = \Delta\varphi(\bar{\lambda})$ is equivalent to guaranteeing zero pressure jump across the free wake.

In a distance ds along the sheet at any fixed t the elemental change in circulation, $d\Gamma$, is determined by this local jump across the sheet of the velocity potential. In fact, for a fixed t ,

$$-d\Gamma = ds \frac{\partial}{\partial s} \Delta\varphi(s, t) = d[\Delta\varphi(\bar{\lambda})] \quad (9)$$

and consequently $d\Gamma = d\Gamma(\bar{\lambda}) \equiv \Gamma'(\bar{\lambda})d\bar{\lambda}$.

In the nonlinear situation $\bar{\lambda}$ plays the convenient role of providing a monotonically increasing "coordinate" along the wake, whether the wake is distorting and rolling-up or not. Thus, for example, the total wake circulation at any given time t is

$$\Gamma_{\text{wake}}(t) = \int_0^{s_{\text{max}}(t)} \gamma_{\text{wake}}(s, t) ds = \int_0^t d\bar{\lambda} \Gamma'(\bar{\lambda}) \quad (10)$$

It is important to note that the variable $\bar{\lambda}$ is *automatically* produced during the computer time-stepping calculations and requires no extra computation. We have found it a very helpful key to the rapid and efficient numerical evaluation of all wake integrals.

Velocity Field of the Wake

Using the variable $\bar{\lambda}$ and complex-variable notation, the plane two-dimensional velocity field associated with the wake can be written from the Biot-Savart Law:^{7,8}

$$u_w(x, y, t) - i v_w(x, y, t) \equiv w_w(z, t) = \frac{1}{2\pi i} \int_0^t d\bar{\lambda} \Gamma'(\bar{\lambda}) \frac{1}{z - z_v(\bar{\lambda}, t)} \quad (11)$$

Here, $z \equiv x + iy$, and $z_v = x_v + iy_v$ is the complex location at time t of the fluid element in the wake having circulation $d\Gamma(\bar{\lambda})$. This "induction integral" is one example of a wake integral that can be determined quite efficiently by taking advantage of the variable $\bar{\lambda}$. For example, we describe in a later paragraph how $\Gamma'(\bar{\lambda})$ is determined via the generalized Wagner equation, whereas the vortex locations $z_v(\bar{\lambda}, t)$ are generated automatically by the code during the time-stepping procedure.^{9,10}

Wake Configurations and Time-Stepping

Figure 1 shows a typical example of a computer-generated version of the vortical wake existing at a given instant t behind an oscillating airfoil as calculated using the techniques implemented in our present code.⁹ This instantaneous configuration is then updated in the following time step, using the velocity associated with both the airfoil bound vorticity and the wake vorticity as in Eq. (11).

The wake configuration shown in Fig. 1 is much like those depicted recently by several authors, and offers no advance over their results. (See, especially, Refs. 11-13 and 15-17 and the references cited therein.) As emphasized by many of these authors, such wake configurations compare well with, and appear to be confirmed by, the shapes of actual nonlinear wakes as observed by flow visualization techniques such as those described in Ref. 14.

In our present computer implementation of the wake convection by time-stepping, in the present code, we have discretized the wake as if it were a sequence of point vortices. As just mentioned, this part of our procedure emulates earlier works and has the same inherent limitations, many of which have been well-documented in the literature.^{11-13,16} In later paragraphs we discuss some of those limitations further, and both our present methods and future plans for either handling or removing some of them.

Airfoil Boundary Conditions

The exact inviscid boundary conditions at the surface of the airfoil can be written down in a form similar to Eq. (3). In this

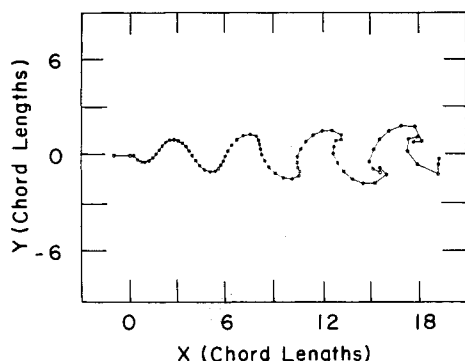


Fig. 1 Wake behind an oscillating airfoil. Typical computer-generated example.

paper we treat the airfoil simply as a flat plate in large-amplitude plunging and pitching motion. The instantaneous position of the airfoil is then described by

$$y|_{\text{airfoil}} = Y_c(x, t) = h(t) - x \tan \alpha(t) \quad (12)$$

where $h(t)$ is the height of the midchord ($x=0$) above the inertial reference axis and $\alpha(t)$ the angle of attack relative to the freestream. Thus, if $\eta_c = y - Y_c(x, t)$, then the no-through-flow boundary condition at the airfoil is $d\eta_c/dt = 0$, yielding

$$v - u \tan \alpha|_{\text{airfoil}} = \dot{h} - x \frac{\dot{\alpha}}{\cos^2 \alpha} \quad (13)$$

or, in the axes fixed to the airfoil itself, (see Fig. 2)

$$\hat{v}|_{\text{airfoil}} = \dot{h} \cos \alpha - \hat{x} \dot{\alpha} \quad (14)$$

If thickness and camber are included in the prescription of the airfoil Eq. (14) is altered somewhat and coupling with the tangential velocity $\hat{u}|_{\text{airfoil}}$ usually occurs. We have recently been able to show that that situation can also be treated by the methods used in this paper.¹⁸⁻²¹ For our present purposes, however, the key features of large amplitude airfoil maneuver are sufficiently well-illustrated by the flat plate example represented by Eq. (14).

Solution for the Velocity Distribution on the Airfoil: Allowing for the Wake

Let us discuss our procedure for satisfying the airfoil boundary condition, Eq. (14), in the light of the classical method used by von Kármán and Sears² and by Wagner.⁵ We adopt a scheme written in the instantaneous coordinates (\hat{x}, \hat{y}) of the airfoil itself, as suggested by Fig. 2. A certain amount of bound vorticity, $\gamma_0(\hat{x}, t)$, would be required on the airfoil to

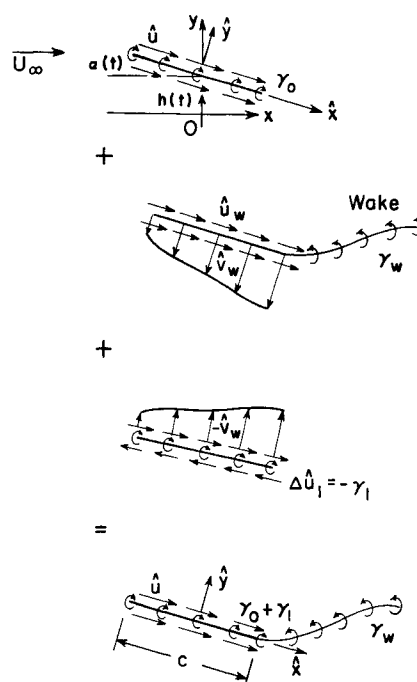


Fig. 2 Conditions at the airfoil: coordinate system and inclusion of the wake effects.

satisfy Eq. (14) is not wake were present. Obtaining γ_0 is a straightforward application of the method of conjugate functions. But additional bound vorticity, $\gamma_1(\hat{x}, t)$, is required to cancel the normal component of the wake-induced velocity [Eq. (11)] at the airfoil.^{2,5} This additional vorticity is obtained by using the steps sketched schematically in Fig. 2 and applying conjugate method to the whole. The *composite* flowfield, associated with the total airfoil vorticity, $\gamma_0 + \gamma_1$, and the wake vorticity, γ_w , then satisfies the requisite boundary conditions at each instant of time.

Using for convenience the angle variable $\beta \equiv \cos^{-1}(2\hat{x}/c)$ we can write the net result for the tangential velocity at the plate as

$$\hat{u}(\beta, t)|_{\text{airfoil}} = U_\infty \cos\alpha + \frac{U_\infty \sin\alpha(1 - \cos\beta)}{\sin\beta} + \hat{u}_w(\beta, t) - \frac{1}{\pi} \left(\frac{1 - \cos\beta}{\sin\beta} \right) \int_0^\pi d\kappa \hat{v}(\kappa, t) \left(\frac{1 + \cos\kappa}{\cos\kappa - \cos\beta} \right) \quad (15)$$

where “ κ ” is a dummy angle variable corresponding to β . In Eq. (15), $\hat{v}(\beta, t)$ is given by

$$\hat{v}(\beta, t) = \dot{h} \cos\alpha - \hat{x}\dot{\alpha} - \hat{v}_w(\beta, t) \quad (16)$$

[Compare Eq. (14)]. Both \hat{u}_w and \hat{v}_w are to be determined from Eq. (11) with z evaluated at the appropriate location on the airfoil surface. Note that $\hat{w}_w \equiv \hat{u}_w - i\hat{v}_w = e^{-i\alpha(t)} w_w$.

Throughout this analysis we have assumed the applicability of the instantaneous Kutta condition at the airfoil trailing edge. The Kutta condition is built in, for example, in the result given in Eq. (15).^{7,8,10}

Mean Velocity and Bound Vorticity on the Airfoil

In the present case [(see Eq. (15))] we see that the mean of the velocities on the top and bottom surfaces, $\langle u(\beta) \rangle \equiv 1/2 [\hat{u}(\beta) + \hat{u}(-\beta)]$, is simply

$$\langle \hat{u}(\beta) \rangle = U_\infty \cos\alpha(t) + \hat{u}_w(\beta) \quad (17)$$

which reduces to the classical linearized theory limit of $\langle \hat{u} \rangle = U_\infty$ for a flat wake and small angle α , since in that limit \hat{u}_w is zero.

The corresponding nonlinear expression for the total airfoil bound vorticity, $-\Delta u(\hat{x}, t)$, at each instant is

$$\gamma(\beta, t) = \gamma_0(\beta, t) + \gamma_1(\beta, t) = -2[U_\infty \sin\alpha(t) - \dot{h} \cos\alpha(t)] \left(\frac{1 - \cos\beta}{\sin\beta} \right) - c\dot{\alpha} \sin\beta - \frac{2}{\pi} \left(\frac{1 - \cos\beta}{\sin\beta} \right) \int_0^\pi \hat{v}_w(\kappa, t) \left(\frac{1 + \cos\kappa}{\cos\kappa - \cos\beta} \right) d\kappa \quad (18)$$

In terms of the definitions used by von Kármán and Sears, γ_0 comprises the first two terms on the *rhs* of Eq. (18) for this case, whereas γ_1 is the final integral term and is associated strictly with the presence of the wake. The corresponding circulations are $\Gamma_0 = \int_{-c/2}^{c/2} d\hat{x} \gamma_0(\hat{x}, t)$ and $\Gamma_1 = \int_{-c/2}^{c/2} d\hat{x} \gamma_1(\hat{x}, t)$.

Wagner's Integral Equation—Nonlinear Version

Wagner's integral equation^{2,5} is used in the classical theory as a relationship between the quasisteady circulation $\Gamma_0(t)$ associated with a given imposed motion of the airfoil and the distribution of the trailing vorticity in the linearized wake. $\Gamma_0(t)$ is the chordwise integral of $\gamma_0(\beta, t)$ [see text, below Eq. (18)]. Thus, with the Kutta condition assumed, it is the bound circulation that would exist if no wake were present. For any given airfoil motion, $\Gamma_0(t)$ is known, so Wagner's equation determines the self-consistent wake vorticity distribution at any instant.

Recalling Kelvin's theorem, we have

$$\Gamma_{\text{airfoil}}(t) + \Gamma_{\text{wake}}(t) = \Gamma(0) \quad (19)$$

where $\Gamma(0)$ is a constant and where, as in Eq. (10), $\Gamma_{\text{wake}}(t)$ is the net circulation in the wake at any instant, obtained by integrating the wake vorticity along the entire wake. On the other hand, in following Ref. 2, we have effectively broken $\Gamma_{\text{airfoil}}(t)$ into two parts:

$$\Gamma_{\text{airfoil}} = \Gamma_0(t) + \Gamma_1(t) \quad (20)$$

where Γ_0 has been defined above and $\Gamma_1 = \int_{-c/2}^{c/2} d\hat{x} \gamma_1(\hat{x}, t)$ is the additional bound circulation (consistent with the Kutta condition) required by the presence of the wake.

When \hat{v}_w , as obtained from Eq. (11), is inserted in the last term of Eq. (18) and the resulting integral expression for Γ_1 is formulated, two of the three integrations can be carried out completely, resulting in an expression for $\Gamma_1(t)$, which involves only a single integration over the wake vorticity. (A key point in this analysis occurs on recognizing the fundamental integral

$$\int_0^{\pi/2} \frac{d\theta}{a + b \cos\theta} = \frac{\pi}{\sqrt{a^2 - b^2}}$$

where in the nonlinear case b is real but a is complex, depending on the location of a given element in the wake. Thus, for this purpose the main mathematical complication introduced by the distortion of the wake is simply the need to keep track of the correct branch of the complex square root.) Then, on eliminating $\Gamma_1(t)$ among Eqs. (19), (20), and (10), we obtain a *nonlinear version* of Wagner's integral equation:

$$\Gamma_0(t) - \Gamma(0) = -Re \left[\int_0^{s_{\max}(t)} ds \gamma_w(s, t) \sqrt{\frac{\hat{z}_v + c/2}{\hat{z}_v - c/2}} \right] \quad (21)$$

or, on using our characteristic variable formulation

$$\Gamma_0(t) - \Gamma(0) = -Re \left[\int_0^t d\bar{\lambda} \Gamma'(\bar{\lambda}) \sqrt{\frac{\hat{z}_v + c/2}{\hat{z}_v - c/2}} \right] \quad (22)$$

where Re indicates “real part.” In Eqs. (21) and (22) the wake vortex location is $\hat{z}_v(\bar{\lambda}, t) = e^{i\alpha} [z_v(\bar{\lambda}, t) - ih(t)]$ in the coordinate system fixed to and moving with the airfoil, and $s_{\max}(t)$ is the distance along the wake from the trailing edge to its end. For the nonlinear case treated in this paper, Eq. (22) is used to determine $\Gamma'(\bar{\lambda})$ in the wake, given $\Gamma_0(t)$ from the specified imposed motion of the airfoil. This enables us to emulate the classical procedure almost exactly. In the linear limit, Eqs. (21) or (22) reduce precisely to Wagner's result.^{5,2}

For the most part, solution of Eq. (22) for the wake vorticity elements is very straightforward, especially during a sequential time-stepping procedure. Once a vortex element has entered the wake, for example, its circulation $\Gamma'(\bar{\lambda}) d\bar{\lambda}$ is “frozen” and needs only be relocated with the element as it convects. Thus, at any time t the entire integral on the *rhs* of Eq. (22) is known, except for the contribution due to the unknown element just entering the wake at that instant. With the *lhs* of Eq. (22) known for the specified motion, the required incremental circulation of the newly entering element is then determined by comparison. One must note, however, that at the beginning of the “starting problem” or after any sudden stop or discontinuity of the imposed motion, careful (analytical) treatment is required because of the singular kernel in Eq. (22),^{9,10,20} and this must be reflected in the code as a conditional branch.

Lift and Moment Formulations

One method of calculating loading, lift, and moment proceeds along relatively standard lines by means of the unsteady

Bernoulli equation. The loading is, for a plate airfoil

$$-\Delta p = \rho_\infty \left[\langle \hat{u}(\beta) \rangle \Delta \hat{u}(\beta) + \Delta \left(\frac{\partial \varphi}{\partial t} \right) \right] \quad (23)$$

One can integrate this loading over the chord to obtain both lift and moment, provided due allowance is made for edge forces. The alternative is to use the principle of conservation of impulse, as emphasized in Ref. 2.

Either way, the results obtained for the large-amplitude case can again be cast in a form remarkably similar to that of the classical theory. We find¹⁰

$$L(t) = L_0(t) + L_1(t) + L_2(t) + \tilde{L}(t)$$

and

$$M(t) = M_0(t) + M_1(t) + M_2(t) + \tilde{M}(t)$$

where the first three terms in each of these expressions have the same physical meaning—and virtually the same form analytically—as their classical counterparts as described by Kármán and Sears.² The terms $\tilde{L}(t)$ and $\tilde{M}(t)$, however, are new: they are *explicitly* nonlinear, have no counterpart in the classical treatment, and formally vanish in the limit of a linearized (low-amplitude) theory.

Specifically, the no-wake terms (sometimes called “quasi-steady” terms) are¹⁰

$$L_0 = -\rho_\infty \bar{U} T_0; \quad M_0 = -\rho_\infty \bar{U} \cos \alpha \int_{-c/2}^{c/2} d\hat{x} \hat{x} \gamma_0(\hat{x}, t) \quad (24)$$

where $\bar{U} \equiv U_\infty + \dot{h} \tan \alpha$. The expression for L_0 is tantamount to applying the Kutta-Joukowski theorem “instantaneously,” with U_∞ replaced by \bar{U} (the apparent freestream speed during plunge) and with the airfoil circulation being obtained as if no wake were present.

L_1 and M_1 represent the apparent mass contributions² and take essentially their classical forms:

$$L_1 = \frac{\rho_\infty}{\cos \alpha} \frac{d}{dt} \int_{-c/2}^{c/2} \hat{x} d\hat{x} \gamma_0; \quad M_1 = \frac{\rho_\infty}{2} \frac{d}{dt} \int_{-c/2}^{c/2} d\hat{x} \gamma_0 \left(\hat{x}^2 - \frac{c^2}{8} \right) \quad (25)$$

even at large amplitudes.

Those remaining terms that are essentially of classical nature are L_2 and M_2 . In particular, L_2 is a wake-induced effect on the lift and is often called the “lift-deficiency” function in the sense that it represents the extent to which the wake’s presence prevents the airfoil from attaining immediately its eventual (“quasisteady”) response to a sudden change in conditions. Knowledge of this lift-deficiency behavior is a key element, for example, in the analysis of airfoil gust response.^{4,5} In the large-amplitude case the results turn out to be¹⁰

$$L_2 = -\frac{\rho_\infty}{\cos \alpha} \frac{c}{2} Re \int_0^t d\bar{\lambda} \Gamma'(\bar{\lambda}) \frac{\frac{\partial \hat{z}_v}{\partial t}}{\sqrt{\hat{z}_v^2 - (c^2/4)}}; \quad M_2 = -\frac{c}{4} L_2 \quad (26)$$

where $\hat{z}_v = \hat{z}_v(\bar{\lambda}, t)$.

It is helpful to note that the wake-integral formulation for L_2 in Eq. (26) is very similar to the classical linear result, with U_∞ in the linear theory being replaced, inside the integral, by the *actual* displacement rate of each vortex element, $\partial \hat{z}_v / \partial t$. In addition, as in Eq. (22), the argument of the square root is complex, again reflecting the displacement of the wake vortex

elements out of the plane of the airfoil. Some of the details of the reductions leading to Eqs. (24–26), together with their comparisons of Kármán and Sears, are available in Refs. 10 and 20.

It is remarkable that $M_2(t)$, even in its nonlinear version, retains the classical property that the lift-deficiency L_2 acts precisely through the airfoil quarter chord.^{3,2}

Finally, the explicitly nonlinear contributions, $\tilde{L}(t)$ and $\tilde{M}(t)$, are found to be

$$\tilde{L}(t) = -\frac{\rho_\infty}{\cos \alpha} \int_{-c/2}^{c/2} d\hat{x} (\gamma_0 + \gamma_1) \hat{u}_w + \frac{\rho_\infty}{\cos \alpha} Re \int_0^t d\bar{\lambda} \Gamma'(\bar{\lambda}) \left(\frac{\partial \hat{z}_v}{\partial t} - \bar{U} \cos \alpha \right) \left(\sqrt{\frac{\hat{z}_v + c/2}{\hat{z}_v - c/2}} - 1 \right) \quad (27)$$

and

$$\tilde{M}(t) = -\rho \int_{-c/2}^{c/2} d\hat{x} \hat{x} (\gamma_0 + \gamma_1) \hat{u}_w + \rho Re \int_0^t d\bar{\lambda} \Gamma'(\bar{\lambda}) \left(\frac{\partial \hat{z}_v}{\partial t} - \bar{U} \cos \alpha \right) \left(\sqrt{\hat{z}_v^2 - \frac{c^2}{4}} - \hat{z}_v \right) \quad (28)$$

Both of these expressions vanish in the linear limit.¹⁰ In practice, for coding purposes, it is useful to convert the first integrals in each of these expressions also into wake integrals.

The conversion of all wake-related quantities in the lift and moment responses to wake integrals is important theoretically because it enables us to verify that the principle of conservation of impulse is satisfied, also in the nonlinear case. But there are also major computational advantages to using the wake integrals. Since the vorticity strengths $\Gamma'(\bar{\lambda})$ are determined by sequential solution of the Wagner equation as we go along, the time-stepping procedure can be used automatically to catalogue all the information needed for evaluation of any of the desired wake integrals. If, at any instant during the run, a lift or moment quantity is required, for example, its evaluation can be called immediately and done explicitly. The efficiency of this procedure is further enhanced by the use of the shifted-time variable $\bar{\lambda}$.

Implementation

The preceding analysis was incorporated initially into a computer program we called NL-WAKE. More recently, an improved code NLJOUK, has been successfully developed.²⁰ In the most recent version of both codes the response of both the wake and the airfoil aerodynamics to given imposed motion are computed by first satisfying the Wagner integral equation at each instant and then evaluating all necessary wake integrals. As noted above, this is tantamount to using impulse theory computationally. In NLWAKE, the free vortex sheet is represented to an array of point vortices, whereas in NLJOUK an additional payed option is made available.²⁰

The advantage of carrying the analysis to the point described in this paper can be seen through the fact that there is only one “unknown” per time step (the value of the additional circulation needed in the wake to maintain the Kutta condition and satisfy Kelvin) when implementing either code. Having obtained this quantity, $\Gamma'(\bar{\lambda})$, via the Wagner equation, all remaining calculations of field and response quantities are explicitly. Not only are no finite-differencing grids required but also, unlike the usual panel methods, for example, no implicit procedures such as matrix inversions are needed. (This approach also works explicitly for Joukowski airfoils of any thickness and camber and also for more general shapes by means of an extension of a method due to Theodorsen. See Refs. 20 and 21.) The “panel method” implemented in NLJOUK, for example, is explicit and is unusual in that sense.

In our present implementation of NLWAKE, for example, the code has a computational time which increases at a rate slightly greater than N^2 , where N is the wake-element discretisation number. Any additional overhead is due to the book-keeping needed for the explicit integration procedures used at any time step.

The computer screen provides an almost ideal tool for depicting and understanding wake evolution in this framework. At each time step each fluid element in the wake (and/or free circulation element) is advanced to its new location in x and y , moving according to $\langle v \rangle$, i.e., in the velocity field of all its neighbors. Since $\bar{\lambda}$ is constant for any such fluid element and t is known, then $\bar{\tau}$ is determined at each new location at each t . In effect, the computer automatically maps the drift time field. When all the fluid elements in a given wake are shown in their new positions at each new time the line through them and the trailing edge at that moment is a streakline that depicts the momentary shape and location of the vortical wake.

The use of an array of point vortices to discretise what is really a smooth vortical wake is well-recognized to be a far from perfect representation.^{11-13,15-17} We nevertheless adopted that approach for the earlier versions of NLWAKE, partly because of its simplicity and partly because of the extensive information now available on how to remedy many of these shortcomings. For example, NLWAKE can, at the user's choice, utilize a variety of desingularization methods^{13,15} and/or "vortex-splitting"¹¹ if needed for a given run. In the end, however, there is a limit to this procedure; it cannot be refined indefinitely.

The fact is that for a point-vortex array the limit of an ever finer time step does not approach the smooth wake even if one could afford it.

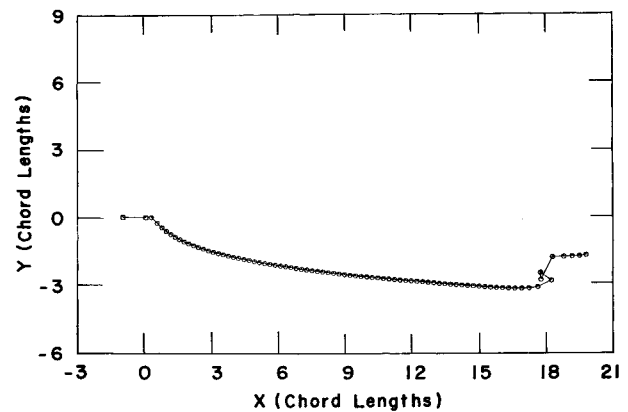
In developing the new code, NLJOUK, therefore, we have implemented an option which uses a stretchable array of vortex panels (including curvature) to represent the wake. A principle feature of this approach is that the limit of finer and finer discretization does approach the smooth continuous wake. The procedure, as coded in NLJOUK, is similar to that used successfully by Hoeijmakers¹⁹ except that the method is explicit, as mentioned above,²⁰ because of our use of the Wagner equation.

Results

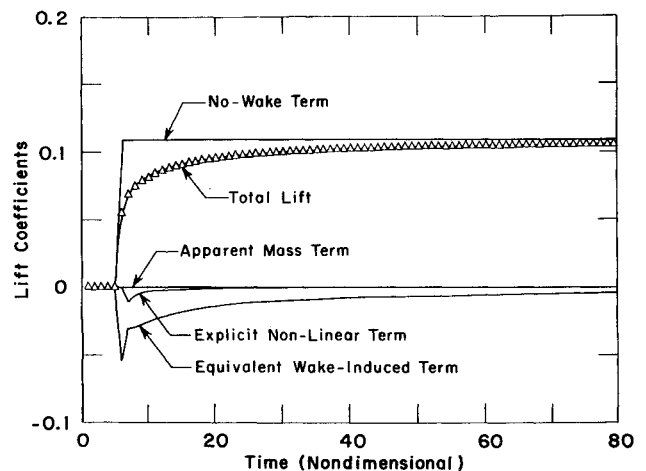
Inputs to either code include the time increment to be used and the desired imposed motion of the airfoil or "maneuver." Analytic or continuous functions are not necessarily required as inputs for the maneuver. The user can create various histories for each of the independent "control" variables $h(t)$ and $\alpha(t)$ by construction, using pieces of functions such as ramps, sinusoids, and steps as building blocks, as desired. Typical results from the program are given in Figs. 3-5 for three basic maneuver elements.

In Fig. 3 we create Wagner's "starting problem" by imposing a step function of magnitude 20 deg in angle of attack at $t = 5$ in order to apply instantaneously a step in the circulation Γ_0 as defined above. Figure 3a is a picture of the wake trace behind the airfoil, after 80 time steps. (The freestream velocity for all examples shown in this paper is equal to $c/4$ per time step.) Figure 3a shows the characteristic roll-up of the starting vortex region as well as the bowing and overall downward displacement of the wake. Improved resolution of the roll-up region can be attained (within the limits mentioned above) by reducing the time step used and/or employing "vortex splitting"^{11,9} as needed.

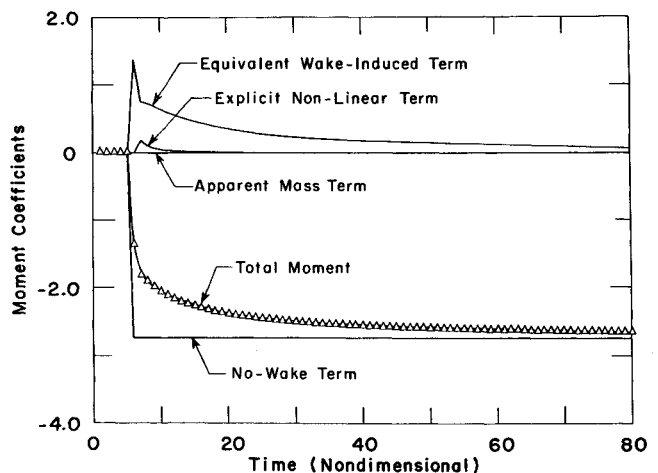
In Fig. 3b, the lift coefficient asymptotes to its steady value as the starting vortex region convects more and more downstream. In addition, the expected instantaneous value of the lift coefficient immediately after the step is recreated.² Just as in the classical linear case, $C_L(t)$ attains half its eventual steady magnitude immediately after the step is imposed. The nose-up pitching moment about the midchord (Fig. 3c) also



a) Wake at $t = 80$



b) History of lift coefficient



c) History of moment coefficient

Fig. 3 The starting problem: instantaneous loading of an airfoil.

shows initial delay relative to its eventual steady value as in the classical theory. In fact, one sees that the lift acts virtually at the one-quarter-chord throughout this "maneuver,"²⁻⁴ consistent with the result in Eq. (26). The small departures observable are due to the "explicitly nonlinear" terms \bar{L} and \bar{M} .

Perhaps the most interesting single feature of this particular example is that not only the qualitative but also the quantitative features of the classical (linearized) results are reproduced, despite the fact that the chosen step amplitude is quite large and large enough to displace the wake downward quite significantly. Even the decay functions for the lift and moment

coefficients differ very little from their linear theory counterparts. In Figs. 3b and 3c various contributions to the total lift and moment coefficients are identified. The "equivalent wake-induced term," for example, is the nonlinear counterpart¹⁰ of the "lift-deficiency" function described by von Kármán and Sears² and is obtained from Eq. (26).

Figures 4 and 5 show sample results for two simple "completed" maneuvers in terms of their effects on the loading of the airfoil. In the first maneuver the airfoil undergoes a sinusoidal oscillation in angle of attack for one complete cycle, then stops its unsteady motion altogether, as shown in Fig. 4a. Figure 4b shows the wake curling up downstream, whereas Fig. 4c shows the effect of the maneuver on the lift coefficient and Fig. 4d shows the response of the moment coefficient. As expected, the lift leads the input function $\alpha(t)$ as a result of the $\dot{\alpha}$ terms. In fact, even the no-wake "Joukowski" lift term, $-\rho_\infty U_\infty \Gamma_0(t)$, contains a leading $\dot{\alpha}$ contribution, since the integral of the first two terms in Eq. (18) gives

$$\Gamma_0(t) = -\pi c U_\infty \sin \alpha - \frac{\pi c^2}{4} \dot{\alpha} \quad (29)$$

with $\dot{h}=0$ and $\alpha(t) = \alpha_0 \sin \omega t$ in this example. [The $\dot{\alpha}$ term in Eq. (29) is sometimes called the "effective camber" due to pitch. It can also be viewed as the lift produced by a twirling paddle in a crosswind.] The result in Eq. (29) provides for this case the lhs driving term for Eq. (22) needed for the determination of the wake-related quantities in the figures; it also appears as the "no-wake term" in Fig. 4c.

Interestingly, the "apparent mass" contribution² to the lift produces, in this example, an additional $\dot{\alpha}$ term of identical sign and magnitude to that in Γ_0 itself. This is also sketched in Fig. 4c.

Both the lift and the moment show the residual effect of the wake's presence after the maneuver has stopped. The residual values of the coefficients, prior to relaxation, are about 5 to 10 percent of the maximum values attained during the maneuver. The sense of the residual value in each case is that of the last completed part of the maneuver. In other words, the motion of the airfoil, in this example is an upward pitch as it completes the sinusoid; this motion sheds counterclockwise vorticity into the wake, which, being nearer to the airfoil than the vorticity shed earlier, creates in turn a net downwash on the airfoil. The downwash diminishes the airfoil's lift and moment relative to their no-wake values, leaving in this example a residual down-load and a residual nose-down moment both of which decay away as the wake vorticity is swept downstream. Once again, one sees the dominant effects of the results in Eq. (26) as the decay proceeds.

The controlling factor for the size and extent of the residual effects appears to be the magnitude of the time rates of change of the input function. This is illustrated for example in Figs. 5a-c, where the input goes to the extreme of a step function in angle of attack followed by the negative of this step 30 time increments later. Figure 5a shows an example of a 10 deg up-and-down step. Note that the resulting wake has a "square wave" appearance, and the residual lift and moment at the end of the maneuver (Figs. 5b and 5c) are on the order of 30 percent of the quasistatic value prior to decay. Step changes, of course, represent very rapid pitching or plunging rates. These high rates introduce large amounts of vorticity into the wake over a short increment of wake length. In the present study, residual lifts and moments of this order are seen in many examples prior to their subsequent decay, and the relaxation process for both the lift and moment often requires many chords lengths of wake convection before the effect of the maneuver is no longer felt.

"Benchmark" Comparisons

From the outset of this study we have sought to establish conclusive "benchmark" comparisons with classical linear

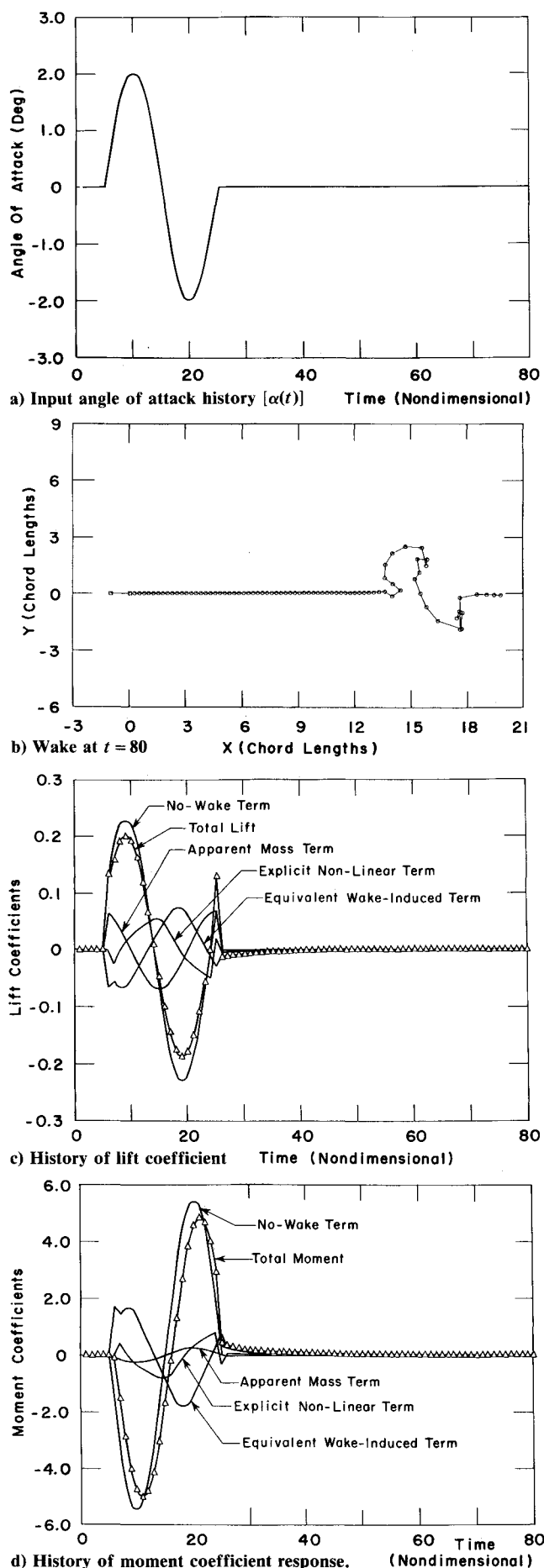
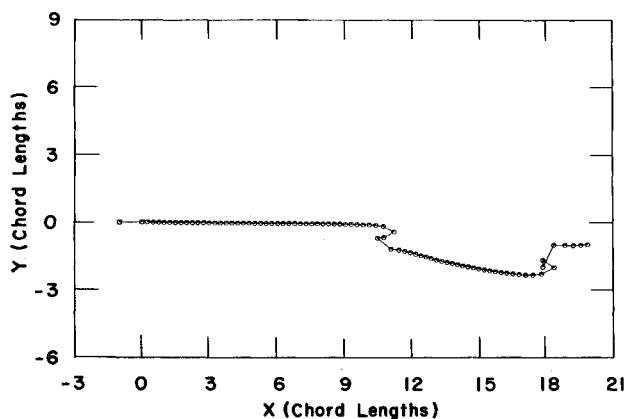
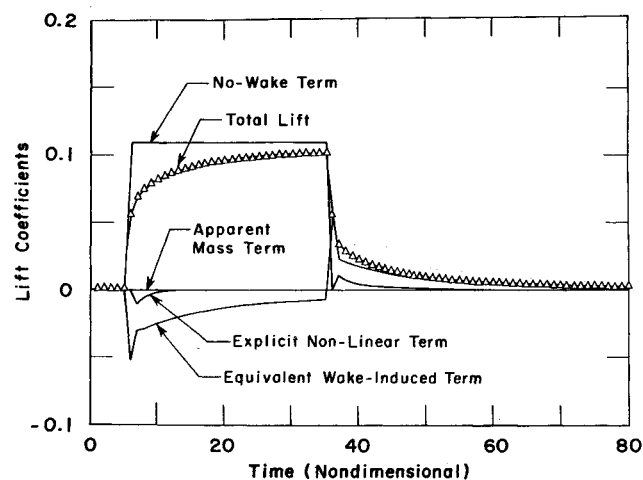
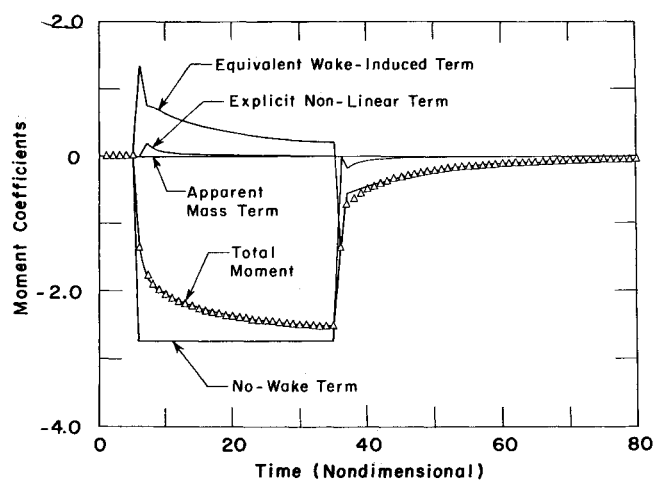


Fig. 4 Sinusoidal maneuver: time variant loading and unloading of an airfoil

a) Wake at $t=80$ 

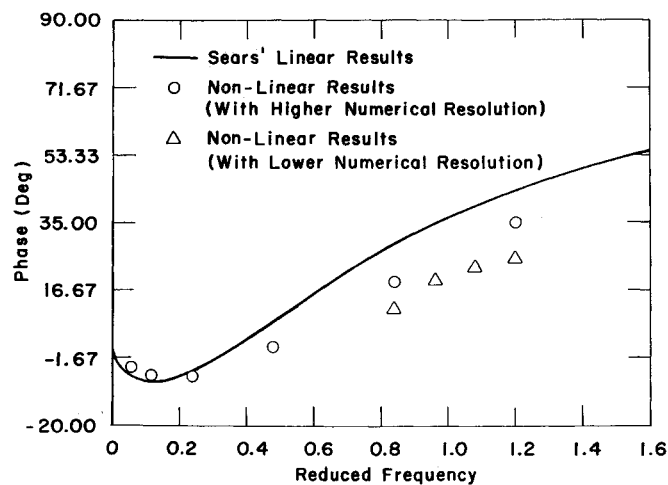
b) History of lift coefficient



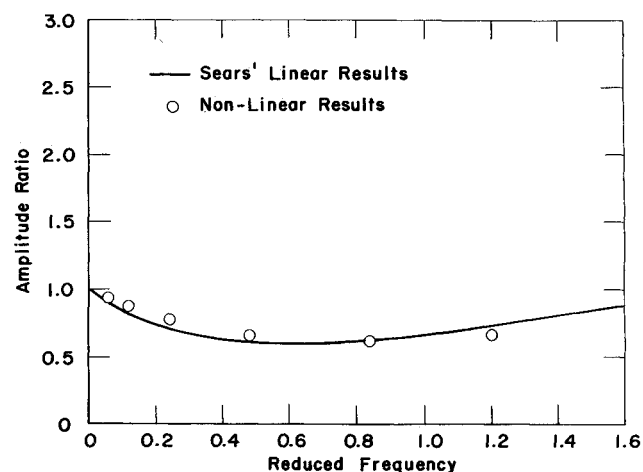
c) History of moment coefficient

Fig. 5 Completed step function "instantaneous" loading and unloading of an airfoil

theory. The response to a step function, as discussed above, was one of those hoped-for benchmarks. A more elusive example has been the numerical determination of the response of an airfoil to continual oscillation in plunge or pitch. We wished to make contact with von Kármán and Sears' linear results,² at least at very low amplitude, comparing our numbers for phase shift and amplitude ratio with the classical answers. However, prior to our use of the wake-integral formulation of the lift and moment response our success was limited. In addition, we verified the expected fact that good wake resolution is necessary for success in a comparison of this sort.



a) Phase change of net lift vs plunging velocity



b) Amplitude ratio of net lift to no-wake lift

Fig. 6 Response of airfoil to steady-state plunging oscillation over a range of reduced frequency $\omega_c/2U_\infty$. Comparison with classical results.

With the wake-integral reformulation, both for NLWAKE and NLJOUK, this benchmark comparison is quite satisfactory, as we show in Fig. 6. In fact, the accuracy based on this comparison now appears to be limited only by the degree of time resolution one is willing or able to use in describing the actual wake evolution.

Figure 6a shows the calculated phase shifts, using the advanced code NLJOUK, for an airfoil oscillating in low-amplitude plunge over a substantial range of reduced frequencies, $\omega_c/2U_\infty$, as compared with the von Kármán-Sears results. Figure 6b illustrates the corresponding amplitude-ratio comparisons. The phase-shift calculations are the most sensitive, as one sees, but we have found that more and more accurate results are systematically obtained as wake resolution is increased. Very similar results are found for the pitching moment response.

The effect of the amplitude of oscillation on the phase shift and amplitude ratio of airfoil response is also investigated and is surprisingly slight, relative to the classical linear theory.

Conclusion

Among the strong points of the present quasi-analytic approach to this problem are the speed and flexibility of the resulting computer codes. Since we solve for only one unknown per time step, the results can be displayed online on a graphics screen. A typical run of NLWAKE of 80 time steps, which may extend the wake 20 chord lengths or more downstream, takes only 5 to 10 min to generate when run on a DEC

VAX 11-750 computer. In terms of flexibility, the programs can be run, especially in the case of NLJOUK, in a high-resolution mode (taking longer, of course) for higher accuracy. The calculations can also accept any combination of sinusoids, pieces of sinusoids, step functions, or constant values in each of the input variables $h(t)$ and $\alpha(t)$. The use is free to "fly" a given maneuver on his or her own, having only to construct a desired realistic forcing function for the airfoil motion with interactive input. The code appears to be particularly valuable in helping to identify and quantify delayed and/or residual aerodynamic responses of airfoils during and after severe maneuver.

Acknowledgments

This study was supported by AFOSR Grants 86-157 and 87-NA-249 and in part by NASA Langley Grant NAG 1-658. The authors also wish to thank Professor Wm. R. Sears for his encouragement and interest in this work and are pleased to dedicate this paper to him in honor of his 75th birthday.

References

- ¹Theodorsen, T., "General Theory of Aerodynamic Instability and the Mechanism of Flutter," NACA Rept. No. 496, 1935.
- ²von Kármán, T. and Sears, W. R., "Airfoil Theory for Non-Uniform Motion," *Journal of Aeronautical Science*, Vol. 5, No. 10, Aug. 1938, pp. 379-390.
- ³Küssner, H. G., "Zusammenfassender Bericht über den Instationären Auftrieb von Flügeln," *Luftfahrtforschung*, Vol. 13, 1936, p. 410.
- ⁴Sears, W. R., "Some Aspects of Non-Stationary Airfoil Theory and its Practical Application," *Journal of Aeronautical Sciences*, Vol. 8, No. 1, 1941, p. 104.
- ⁵Wagner, H., "Dynamischer Auftrieb von Tragflügeln," *Zeitschrift für Angewandte Mathematik und Mechanik*, Vol. 5, 1925, p. 17.
- ⁶Lamb, H., *Hydrodynamics*, 6th ed., Dover, New York, 1945.
- ⁷Milne-Thompson, L. M., *Theoretical Aerodynamics*, Dover, New York, 4th ed., 1973, Chapters 5-7.
- ⁸Prandtl, L. and Tietjens, O. G., *Fundamentals of Hydro- and Aeromechanics*, Dover, New York, 1st ed., 1957, pp. 176-178.
- ⁹Scott, M. T., "Nonlinear Airfoil-Wake Interaction in Large Amplitude Unsteady Flow," M.S. Thesis, Dept. of Aeronautics and Astronautics, Massachusetts Institute of Technology, Cambridge, MA, Aug. 1987.
- ¹⁰McCune, J. E., "Unsteady Wing Theory: The Kármán/Sears Legacy," AIAA Paper 88-3540, July 1988.
- ¹¹Mook, D. T., "On the Numerical Simulation of the Unsteady Wake Behind an Airfoil," AIAA Paper 87-0190, Jan. 1987.
- ¹²Pullin, D. I. and Jacobs, P. A., "Inviscid Evolution of Stretched Vortex Arrays," *Journal of Fluid Mechanics*, Vol. 171, Oct. 1986, pp. 377-406.
- ¹³Stremel, P. M., "A Method for Modeling Finite Core Vortices in Wake Flow Calculations," AIAA Paper 84-0417, Jan. 1984.
- ¹⁴Van Dyke, M., *An Album of Fluid Motion*, Parabolic, Stanford, CA, 1982, pp. 56-57.
- ¹⁵Katz, J. and Weihs, D., "Behavior of Vortex Wakes from Oscillating Airfoils," *Journal of Aircraft*, Vol. 15, No. 12, 1978, pp. 861-863.
- ¹⁶Katz, J. and Weihs, D., "Wake Rollup and Kutta Conditions for Airfoils Oscillating at High Frequency," *AIAA Journal*, Vol. 19, No. 12, 1981, pp. 1604-1606.
- ¹⁷Levin, D. and Katz, J., "Vortex-Lattice Method for the Calculation of the Nonsteady Separated Flow Over Delta Wings," *Journal of Aircraft*, Vol. 18, No. 12, 1981, pp. 1032-1037.
- ¹⁸McCune, J. E. and Tavares, T. S., "Unsteady 3D Aerodynamics of Slender Wings in Severe Maneuver," AIAA Paper 88-3544, July 1988.
- ¹⁹Hoeijmakers, H. W. M., "An Appropriate Method for Computing Inviscid Vortex Wake Roll-Up," National Aerospace Laboratory, Amsterdam, the Netherlands, NLR TR-85149 U, 1985.
- ²⁰Lam, C.-M. G., "Nonlinear Wake Evolution of Joakowski Airfoils in Severe Maneuver," MIT M.Sc. Thesis, June 1989.
- ²¹Benson, H., "Apparent-Mass and On-Board Circulation of Joakowski Airfoils and Cascades in Severe Unsteady Motion," MIT M.Sc. Thesis, May 1989.